JOURNAL OF OPTOELECTRONICS AND ADVANCED MATERIALS Vol. 9, No. 8, August 2007, p. 2638 - 2643

Phototransport and photoluminescence in nanocrystalline porous silicon

V. IANCU, M. L. CIUREA[*,a], I. STAVARACHE[a], V. S. TEODORESCU[a]
Department of Physics, University "Politehnica" of Bucharest, Bucharest 060042, Romania
[a]National Institute of Materials Physics, 077125 Bucharest - Măgurele, P.O. Box MG-7, Romania

The paper presents the phototransport and photoluminescence investigations on nanocrystalline porous silicon. Spectral dependence curves of the phototransport and photoluminescence were taken at room temperature. A typical phototransport curve presents several maxima and shoulders, while the photoluminescence curves present only one maximum. The temperature dependence of the phototransport was measured in the 85 – 250 K range for different wavelengths. All these curves present only one activation energy on the whole temperature interval. The experimental results are interpreted taking into account a quantum confinement model. Previous microstructure investigations proved that the studied nanocrystalline porous silicon is formed by a nanowire network. Then, the electron Hamiltonian can be split into the sum of a 1D longitudinal Bloch part and a 2D transversal part, the nanowire wall acting like a potential well. Thus, a number of discrete energy levels will appear into the band gap. Both phototransport and photoluminescence maxima are due to the transitions between these levels, corresponding to a mean nanowire diameter of 3.2 nm, in good agreement with the previous microstructure and electrical transport investigations. On the contrary, the temperature dependence of the phototransport is determined by the surface states located on the internal surface and/or the interface between nanocrystallites.

(Received January 15, 2007; accepted June 27, 2007)

Keywords: Nanocrystalline porous silicon, Phototransport, Photoluminescence, Quantum confinement

1. Introduction

The nanomaterials and nanostructures present a great interest for the modern science and technology. The properties and phenomena specific to these materials and structures are mainly due to the quantum confinement (QC), which is determined by the sizes of 10 – 20 interatomic distances, and to the surface/interface effects, which are amplified by the enormous surface/volume ratio (10^8 – 10^9 m^{-1}). Consequently, new applications of the nanomaterials appear (e.g. photodetectors [1 – 3]). Compared to other nanostructured materials, the nanosilicon presents the double advantage of cheap price and compatibility with the bulk silicon. The nanosilicon is intensely photoluminescent in the visible range at room temperature (RT) and it is extremely sensitive to the ambient composition, leading to possible optoelectronic, biomedical and sensor applications [4 – 11].

Many experimental investigations lead to the conclusion that the photoluminescence (PL) of the nanocrystalline silicon is mainly due to the QC, while its surface/interface contribute to the passivation of non-radiative states and the formation of radiative recombination states [4 – 7, 12 – 14]. This is why it is of great interest to investigate the role of the QC in photoelectrical phenomena, especially in phototransport (PT). PT was scarcely studied in nanomaterials and nanostructures, both silicon-based [3, 15 – 18] or with different compositions [1, 2].

Our team has systematically investigated the role of the QC in the electrical transport through nanocrystalline porous silicon (nc-PS) [19 – 22] and Si – SiO_2 nanocomposites [22, 23]. In the following we will discuss the role of the QC in PT and PL processes. Section 2 deals with the experimental investigations. Section 3 presents the QC model. Section 4 analyzes the PT and PL experimental results within the frame of the model and the last Section presents the conclusions.

2. Experimental

The investigated nc-PS layers were prepared from p-type (100) Si wafers (5 – 15 Ω·cm resistivity) [19, 20, 24]. At first, the wafers were electrochemically etched in HF (49 %) – C_2H_5OH (1:1 volume ratio) under constant current density (5 – 25 mA/cm^2). After this, they were photochemically etched (by illuminating them *in situ* with a Xenon lamp for 1.5 – 3 min), cleaned in double distilled water and dried in air (two weeks), to obtain fresh samples. The samples were then stabilized by oxidation, either native (storage in ambient conditions for at least 1.5 years) or anodic.

The microstructure investigations, performed with a TEMSCAN JEOL 200CX analytic electron microscope and a high resolution TOPCON 002B microscope, proved that the nc-PS layers are formed by a system of alveolar columnar macropores (1.5 – 3 μm diameter), practically orthogonal on the layer surface (see Fig. 1), while the alveolar walls (100 – 200 nm thickness) are formed by a nanowire network (1 – 5 nm diameter, 5 – 35 μm length, see Fig. 2) [20, 25].

Invited paper at International Conference ROCAM'06, September 2006, Bucharest, Romania

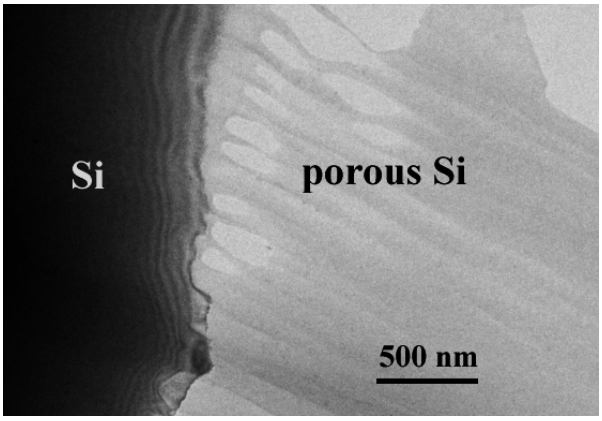

Fig. 1. Low magnification XTEM image of the Si/nc-PS interface.

The spectral dependence of the PT at RT and the temperature dependence of the PT at different wavelengths (500 nm, 575 nm and 600 nm) were measured for different constant biases in 1 – 20 V range, using an Agilent E3631A d.c. power supply. A 100 W incandescence lamp was used as light source. The wavelengths were selected through Karl Zeiss Jena interferential filters in 1,100 – 425 nm range, with the wavelengths varying in steps of 25 nm. The filters were preferred to a monochromator, because their transmittance is at least 20 times bigger and therefore they allow the observation of small peaks. The sample was placed on the finger of a cryostat with optical windows (12,000 – 400 nm range). The photocurrent was measured with a Keithley 642 electrometer and was normalized to the spectral distribution of the source and the transmittance of the filters. Both coplanar (distance between parallel Al electrodes 2 and 3 mm, respectively) and sandwich (bottom Al / c-Si / PS / semitransparent top Al) configurations were used. In the case of the sandwich configuration, the photocurrent was also normalized to the transmittance of the semitransparent Al electrode (325 nm thickness). All the measurements were computer-assisted.

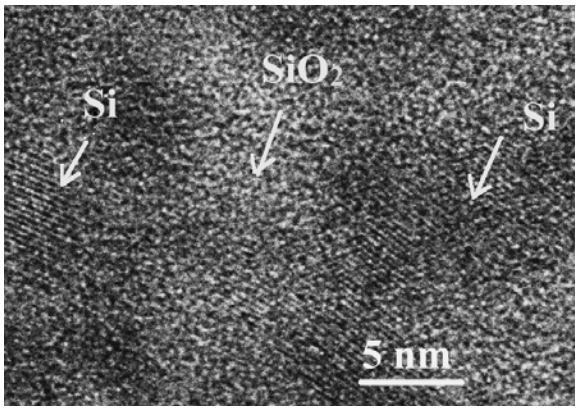

Fig. 2. High resolution XTEM image of the nc-PS nanowire network.

The spectral dependence of the PL at RT was measured with a computer-assisted EMI 9558 QB photomultiplier (cooled at –15 ^{o}C with Peltier elements), through a SPEX double monochromator. The sample was excited with a 500 W mercury lamp, the 334 nm wavelenght being selected through a SPM-2 monochromator with quartz prism, an interferential filter and a GG13 Schott filter.

3. Results

3.1. Phototransport

Figs. 3 – 5 present the spectral dependence of the PT at RT measured in coplanar configuration. The curve from Fig. 3 was measured on an anodically oxidized sample (3 mm distance between electrodes). The curves from Figs. 4 and 5 were measured on a sample fully stabilized by native oxidation (2 mm distance between electrodes). The results of the measurements performed in sandwich configuration, on partially stabilized samples (native oxidation for 7 months) are shown in Figs. 6 and 7. As one can see, all the curves have maxima and/or shoulders at practically the same wavelengths, listed in Table 1. The experimental error in the wavelength is ± 12.5 nm. Therefore one can identify a maximum from only three points, the relative error being smaller than 2.5 %. The experimental error in the photocurrent intensity is about 1 % from the value of the absolute maximum of each curve (smaller than the vertical size of the experimental points in Figs. 3 – 7). Then, even an apparently small maximum is significant. We have to mention that the measurements were made on several samples prepared in the same conditions and the results are fully reproducible. One can observe that the maximum quoted with F (from false) appears as a small shoulder in only one characteristic, so that it will be neglected in the following (as an experimental error). At the same time, one can see that the relative amplitude of the maxima depends on the applied bias.

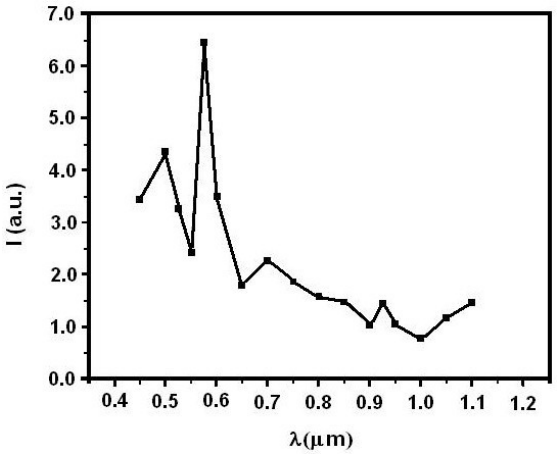

Fig. 3. Spectral distribution of the photocurrent: coplanar structure, anodical oxidation, U = 1.5 V.

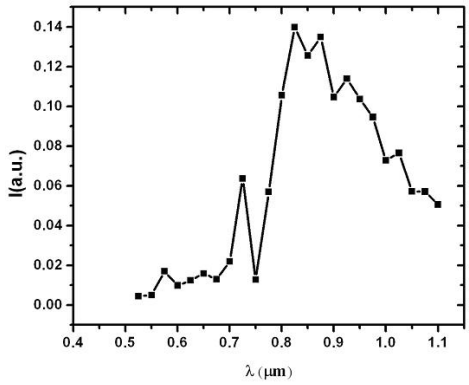

Fig. 4. Spectral distribution of the photocurrent: coplanar structure, native oxidation, U = 1 V.

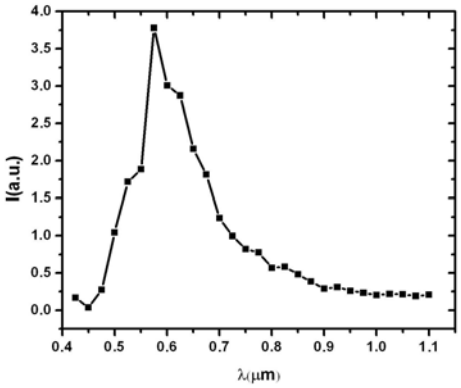

Fig. 6. Spectral distribution of the photocurrent: sandwich structure, native oxidation, U = 1 V.

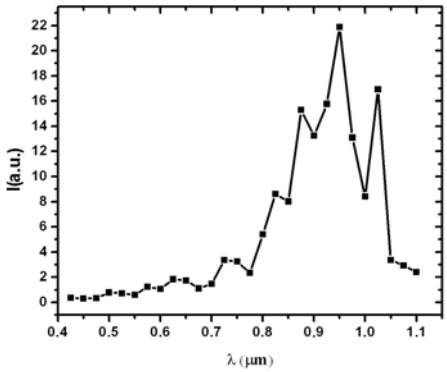

Fig. 5. Spectral distribution of the photocurrent: coplanar structure, native oxidation, U = 20 V.

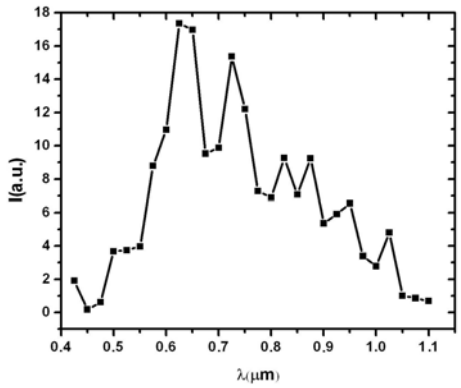

Fig. 7. Spectral distribution of the photocurrent: sandwich structure, native oxidation, U = 20 V.

Table 1. Photocurrent maxima at RT.

No.	Parameters	Coplanar			Sandwich		Mean value
		d = 3 mm	d = 2 mm				
		U = 1.5 V	U =1 V	U = 20 V	U =1 V	U = 20 V	
1.	λ (nm)	500		500	525	500	506
	E (eV)	2.48		2.48	2.36	2.48	2.45
2.	λ (nm)	575	575	575	575	575	575
	E (eV)	2.16	2.16	2.16	2.16	2.16	2.16
3.	λ (nm)		650	625	625	625	631
	E (eV)		1.91	1.98	1.98	1.98	1.96
4.	λ (nm)	700	725	725		725	719
	E (eV)	1.77	1.71	1.71		1.71	1.72
F.	λ (nm)				775		
	E (eV)				1.60		
5.	λ (nm)		825	825	825	825	825
	E (eV)		1.50	1.50	1.50	1.50	1.50
6.	λ (nm)		875	875		875	875
	E (eV)		1.42	1.42		1.42	1.42
7.	λ (nm)	925	925	950	925	950	935
	E (eV)	1.34	1.34	1.31	1.34	1.31	1.33
8.	λ (nm)		1.025	1.025		1.025	1.025
	E (eV)		1.21	1.21		1.21	1.21

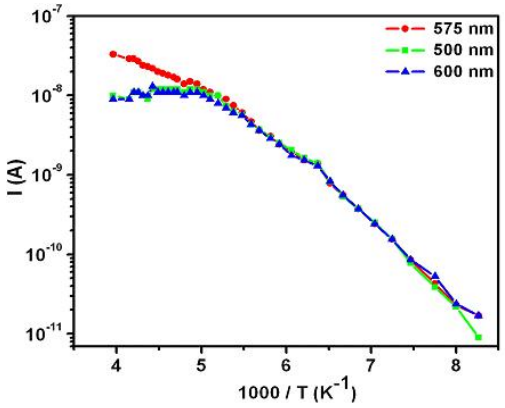

Fig. 8. Temperature dependence of the photocurrent: coplanar structure, anodical oxidation, U = 1.5 V.

The temperature dependence of the PT is shown in Fig. 8. One can see that, for all the investigated wavelengths, one has a single activation energy (E_a = 0.21 eV). This value is much smaller than both the PT maxima discussed above and the activation energies previously measured in the temperature dependence of the dark current [19], but comparable with the surface trapping levels [19, 26 – 28].

3.2. Photoluminescence

The PL curve (Fig. 9) presents a single broad maximum, at λ = 656 nm (E = 1.89 eV), the FWHM being 250 nm (0.72 eV). The curve has a gaussian shape, similar with the size distribution of the nanowires [20].

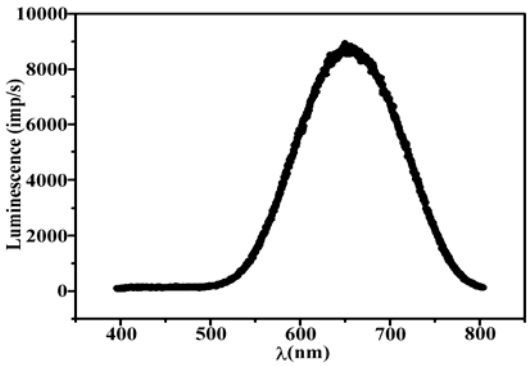

Fig. 9. Spectral distribution of the PL at RT.

4. Modelling

In order to find out the role played by the QC in PT phenomena, one has to remind that the simplest way to describe the QC is to consider that the nanocrystal surface acts like the wall of a potential well. Several kinds of potential wells were investigated rectangular (either finite or infinite) [19 – 23, 25, 29, 30], parabolic [31], Woods-Saxon [32] etc. For the modeling of the QC in PT, the rectangular infinite potential well is accurate enough (less than 5 % errors for the first four levels, compared with the finite well of minimum 2 eV depth and minimum 2 nm width [19, 20, 25, 29]) with respect to the experimental dispersion due to the size and shape dispersion of the nc-PS nanocrystallites.

In the case of the studied nc-PS samples (formed by a nanowire network [20, 25]), one can admit that the nanowires have cylindrical symmetry (as a first approximation). Due to the great length/width ratio, the electron Hamiltonian can be split into the sum of a 1D (Bloch type) longitudinal part and a 2D (infinite cylindrical well) transversal part. Then, the electron energy is

$$E = \varepsilon_{n,k_z} + \frac{2\pi^2\hbar^2}{m^* d^2} x_{l,p}^2 = \left(\varepsilon_{n,k_z} + \frac{2\pi^2\hbar^2}{m^* d^2} x_{0,l}^2\right) + \frac{2\pi^2\hbar^2}{m^* d^2}\left(x_{l,p}^2 - x_{0,l}^2\right) \equiv \varepsilon_{n,k_z}^s + E_{l,p-l} \tag{1}$$

where

$$E_{l,p} = \frac{2\pi^2\hbar^2}{m^* d^2}\left(x_{l,p+1}^2 - x_{0,1}^2\right) \tag{2}$$

is the QC energy level, with $z_{l,p} = \pi \cdot x_{l,p}$ as the p-th zero of the Bessel function $J_l(z)$, l being the orbital quantum number, ε_{n,k_z}^s is the longitudinal Bloch energy, shifted to have $E_{0,0} \equiv 0$, $m^* = 0.66 \cdot m_e$ is the transversal effective electron mass and d the nanowire diameter.

The application of the model to the temperature dependence of the dark current [19, 20, 25, 29] proved that the cylindrical approximation leads to errors of about 2.57 %. We have also analyzed the square prism symmetry [20, 25], but it leads to errors of about 13.6 %, so that in the following we will use the cylindrical symmetry only.

The relations (1), (2) are valid in the effective mass approximation, where the energy – diameter relation is of the form $E \propto d^{-2}$. This is no longer correct at nanometer scale [33, 34], where the LCAO calculations lead to a $E \propto d^{-1.02}$ dependence [33]. However, if one admits that the effective mass becomes size-dependent [35], the effective mass approximation still holds.

5. Discussion

As the samples are practically stabilized after 1.5 years [19, 25] and the diameter reduction through oxidation is one interatomic distance [19, 20, 25], one can expect that the mean diameters of the nanowires from the different investigated samples are practically equal. If one admits that the mean diameter is $d \cong 3.25$ nm (in agreement with the previous microstructure and electrical transport investigations [19, 20, 25]), one can interpret almost all the observed PT maxima as due to optical transitions between QC levels (under the condition $\Delta l = \pm 1$). For instance, the first maximum from Table 1 (E_1 =

2.45 eV) will correspond to the (2, 3) → (1, 2) transition. We have quoted (l, p) the QC level with energy $E_{l,p}$. If one introduces the relative error of the transition energy as

$$\sigma_r = \frac{E_{\exp}}{\Delta E_{teor}} - 1, \quad (3)$$

one finds $\sigma_r = -3.03\,\%$ for this first maximum. The identification of the quantum transitions and the corresponding errors are presented in Table 2.

One can see that the maximum No. 6 (λ = 875 nm, E_6 = 1.42 eV) cannot be identified with a QC transition. The fact that this maximum appears only in native oxidized samples suggests that it corresponds to a Si/SiO_2 interface state, due to the imperfections of the native oxide. At the same time, one has to underline the low errors, of the same order of magnitude as the QC model errors. At the same time, the sum of the relative errors is – 1.69 % for d = 3.25 nm and + 2.61 % for d = 3.26 nm, confirming the chosen diameter value (3.25 nm).

Table 2. QC transitions identified in PT measurements.

No.	E_{exp} eV)	Transition	σ_r (%)
1	2.45	(2, 3) → (1, 2)	– 3.03
2	2.16	(1, 2) → (0, 0)	+ 0.99
3	1.96	(0, 3) → (1, 1)	– 0.30
4	1.72	(1, 2) → (2, 0)	+ 1.83
5	1.50	(3, 1) → (2, 0)	– 0.54
6	1.42	–	–
7	1.33	(0, 2) → (1, 0)	+ 0.93
8	1.21	(2, 1) → (1, 0)	– 1.57

The bias dependence of the relative amplitude of the PT maxima can also be interpreted as due to the QC. Indeed, the light penetration depth increases with the wavelength. Due to the microstructure of the investigated nc-PS samples, the number of carriers at a given depth is finite (and small, due to the Coulomb blockade effect [21]). Consequently, the number of non-equilibrium carriers generated by illumination increases with the penetration depth, instead of decreasing (like in bulk samples). This is also in agreement with the differences observed between the coplanar and sandwich structures, induced by the geometry of the electric field.

The activation energy of the temperature dependence of the PT (0.21 eV) can also be identified with a transition, namely (1, 0) → (0, 0). The relative error is σ_r = + 5.00 %. If one compares it with the shallow surface trapping level (0.29 eV, see [19]), one obtains a relative error of – 27.59 %. Therefore, the identification with the (1, 0) → (0, 0) transition is acceptable.

The PL maximum corresponds to the (2, 2) → (1, 1) transition ($\sigma_r = +0.43\,\%$). It can also be observed that, due to the small differences between different transitions and the great width of the maximum, it can also be identified with the (0, 3) → (1, 1) transition observed in PT (maximum No. 3), with an error $\sigma_r = -3.86\,\%$. This proves that PL is mainly due to the QC, in agreement with the previous studies [4 – 7, 12 – 14].

Several experimental investigations and models for the PL and PT in PS were presented in the literature. Svechnikov, Kaganovich and Manoilov [36] obtained photosensitivity maxima for PS situated between 400 and 500 nm. Pridmore [37] performed near field measurements and reaches the conclusion that the PL for his PS samples is due to the surface states only. Averkiev, Kazakova and Smirnova [38] use a space charge model with anomalous diffusion and obtain a characteristic energy of 0.03 eV (situated completely out of any experimental range for PS yet observed in any kind of investigations). Sehrawat and Mehra [39] analyze the role of the non-radiative recombination in PT and prove the blue shift of the photocurrent maximum with the crystallite size decrease. Brügemann [40] proposes a numerical model for the transient regime of the PT. One can observe that some of these results [36, 39] are in agreement with ours, while others [37, 38] are essentially different. It seems that the differences are due to the different ways of preparing the PS, leading to different behaviours.

6. Conclusions

To summarize, we have obtained 8 maxima (and shoulders) in the PT measurements made on nc-PS (situated at 506, 575, 633, 715, 825, 875, 935, and 1,025 nm, with an experimental error of ± 25 nm) and one broad PL maximum (situated at 656 ± 125 nm).

We have proved that the position of the maxima in the PT measurements does not depend on either the amplitude or the geometry of the applied electric field, while their relative amplitudes are strongly dependent on both of them.

All PT maxima but one, as well as the PL maximum can be identified as corresponding to optical transitions between QC levels. The relative errors induced by this identification are of the same order of magnitude as the errors of the model used to compute the QC levels.

The PT maximum observed at λ = 875 nm (E_6 = 1.42 eV) cannot be identified with any reasonable precision with a QC transition and it seems that it corresponds to a Si/SiO_2 interface state, due to the imperfections of the native oxide (as it was observed only in natively oxidized samples).

The temperature dependence of the PT shows only one activation energy for all the investigated wavelengths. Its value (0.21 eV) was identified with the (1, 0) → (0, 0) transition, the relative error being + 5.00 %.

Acknowledgements

This work was partially supported from the CERES C4-169/2004 Project, in the frame of the National Plan for Research and Development.

References

[1] A. C. Arango, A quantum dot heterojunction photodetector, M. Sc. Thesis, MIT 2005.
[2] S. A. McDonald, P. W. Cyr, L. Levina, E. H. Sargent, Appl. Phys. Lett. **85**, 2089 (2004).
[3] A. I. Yakimov, A. V. Dvurechenskii, Yu. Yu Proskuryakov, A. I. Nikiforov, O. P. Pchelyakov, S. A. Teys, A. K. Gutakovskii, Appl. Phys. Lett. **75**, 1413 (1999).
[4] B. Hamilton, Semicond. Sci. Technol. **10**, 1187 (1995).
[5] A. G. Cullis, L. T. Canham, P. D. J. Calcott, J. Appl. Phys. **82**, 909 (1997).
[6] Properties of Porous Silicon, edited by L. T. Canham, EMIS Datareviews Series No. 18, INSPEC, London (1997).
[7] Semiconductors and Semimetals, vol.49 – Light Emission in Silicon: From Physics to Devices, edited by D. J. Lockwood, Academic Press, San Diego (1998).
[8] M. Brewer, U. Utzinger, Y. Li, E. N. Atkinson, W. Satterfield, N. Auersperg, M. Follen, R. Bast, J. Biomed. Optics **7**, 20 (2002).
[9] D. A. LaVan, T. McGuire, R. Langer, Nature Biotechnology **21**, 1184 (2003).
[10] Z. Gaburro, C. J. Oton, L. Pavesi, Appl. Phys. Lett. **84**, 4388 (2004).
[11] Z. Gaburro, P. Bettotti, M. Saiani, L. Pavesi, Appl. Phys. Lett. **85**, 555 (2004).
[12] X. J. Li, Y. H. Zhang, Phys. Rev. B **61**, 12605 (2000).
[13] S. Tripathy, R. K. Soni, S. K. Ghoshal, K. P. Jain, Bull. Mater. Sci. **24**, 285 (2001).
[14] R. Prabakaran, R. Kesavamoorthy, A. Singh, Bull. Mater. Sci. **28**, 219 (2005).
[15] M. Ando, T. Kobayashi, H. Naito, T. Nagase, Y. Kanemitsu, Thin Solid Films **499**, 119 (2004).
[16] N. Koshida, H. Koyama, Appl. Phys. Lett. **62**, 1617 (1993).
[17] M. R. Reshotko, I. Balberg, Appl. Phys. Lett. **78**, 763 (2001).
[18] S. Lettieni, G. Di Francia, Phil. Mag. (B) **81**, 133 (2001).
[19] M. L. Ciurea, I. Baltog, M. Lazar, V. Iancu, S. Lazanu, E. Pentia, Thin Solid Films **325**, 271 (1998).
[20] M. L. Ciurea, V. Iancu, V. Teodorescu, L. Nistor, M. G. Blanchin, J. Electrochem. Soc. **146**, 3516 (1999).
[21] M. L. Ciurea, M. Draghici, V. Iancu, M. Reshotko, I. Balberg, J. Luminesc. **102-103**, 492 (2003).
[22] M. L. Ciurea, J. Optoelectron. Adv. Mater. **7**, 2341 (2005).
[23] M. L. Ciurea, V. S. Teodorescu, V. Iancu, I. Balberg, Chem. Phys. Lett. **423**, 225 (2006).
[24] M. L. Ciurea, E. Pentia, A. Manea, A. Belu-Marian, I. Baltog, Phys. Stat. Sol. (b) 195, 637 (1996).
[25] M. L. Ciurea, V. Iancu, Proc. IEEE CN 00TH8486, Int. Semicond. Conf. CAS 2000, Sinaia, 6 – 9 October 2000, 1, 55 (2000).
[26] M. L. Ciurea, M. Draghici, S. Lazanu, V. Iancu, A. Nasiopoulou, V. Ioannou, V. Tsakiri, Appl. Phys. Lett. **76**, 3067 (2000).
[27] M. Draghici, M. Miu, V. Iancu, A. Nassiopoulou, I. Kleps, A. Angelescu, M. L. Ciurea, Phys. Stat. Sol. (a) **182**, 239 (2000).
[28] V. Iancu, M. L. Ciurea, Mihai Draghici, J. Appl. Phys. **49**, 216 (2003).
[29] V. Iancu, M. L. Ciurea, Sol. St. Electron. **42**, 1893 (1998).
[30] M. L. Ciurea, J. Optoelectron. Adv. Mater. **8**, 13 (2006).
[31] W. P. Yuen, Phys. Rev. B **48**, 17316 (1993).
[32] K. Clemenger, Phys. Rev. B **44**, 12991 (1991).
[33] C. Delerue, G. Allan, M. Lannoo, Phys. Rev. B **48**, 11024 (1993).
[34] J. Heitmann, F. Müller, L. X. Yi, M. Zacharias, D. Kovalev, F. Eichhorn, Phys. Rev. B **69**, 195309 (2004).
[35] J. Wang, A. Rahman, A. Ghosh, G. Klimeck, M. Lundstrom, IEEE Trans. Electron Dev. **52**, 1589 (2005).
[36] S. V. Svechnikov, E. B. Kaganovich, E. G. Manoilov, Semicond. Phys., Quantum Electron. & Optoelectron. **1**, 13 (1998).
[37] A. Pridmore, American Physical Society Centennial Meeting, Session FC17 - Near Field Microscopy, FC17.08, Atlanta, March 20 – 26, 1999.
[38] N. S. Averkiev, L. P. Kazakova, N. N. Smirnova, Semiconductors **36**, 336 (2002).
[39] Kiran Sehrawat, R. M. Mehra, Indian J. Pure & Appl. Phys. **41**, 495 (2003).
[40] R. Brüggemann, Phys. Stat. Sol. C **1**, 1227 (2004).

* Corresponding author: ciurea@.infim.ro